

On Estimating the Probabilistic Region of Attraction for Partially Unknown Nonlinear Systems: An Sum-of-Squares Approach

Hejun Huang¹, Dongkun Han²

1. Department of Mechanical and Automation Engineering, The Chinese University of Hong Kong, HKSAR, China
E-mail: hjhuang@mae.cuhk.edu.hk

2. Department of Mechanical and Automation Engineering, The Chinese University of Hong Kong, HKSAR, China
E-mail: dkhan@mae.cuhk.edu.hk

Abstract: Estimating the region of attraction for partially unknown nonlinear systems is a challenging issue. In this paper, we propose a tractable method to generate an estimated region of attraction with probability bounds, by searching an optimal polynomial barrier function. Chebyshev interpolants, Gaussian processes and sum-of-squares programmings are used in this paper. To approximate the unknown non-polynomial dynamics, a polynomial mean function of Gaussian processes model is computed to represent the exact dynamics based on the Chebyshev interpolants. Furthermore, probabilistic conditions are given such that all the estimates are located in certain probability bounds. Numerical examples are provided to demonstrate the effectiveness of the proposed method.

Key Words: Region of attraction, Sum-of-squares programming, Chebyshev interpolants, Gaussian processes.

1 Introduction

Tracking the performance of uncertain nonlinear systems is an essential problem of significant research interests. In engineering practices, the concepts of safety and stability are central to these uncertain nonlinear systems in most scenarios, e.g., flight dynamics, bipedal robotics and power systems [1–4]. Consequently, scientists across multiple disciplines have summarized this type of problem into the analysis of region of attraction (ROA, also called domain of attraction). Estimating the ROA can directly obtain the safety or the stability margin in many real implementations [5].

Fruitful results have been obtained to estimate the ROA of fixed nonlinear systems. Exploiting the sublevel set of Lyapunov functions is one of the widely used methods [6]. Barrier functions are another powerful tool to guarantee safety such that states never enter into a specified unsafe region [7], [8]. To meet the safety and the stability conditions simultaneously, the quadratic programs have been investigated to find qualified Lyapunov barrier functions [9]. Meanwhile, sum-of-squares programmings (SOSPs) are proposed to find more permissive functions in polynomial systems [10–13]. However, it is not infrequent to observe model inaccuracies and unknown disturbances that might influence the system dynamics or even result in operation failures in the worst case. To handle with the above issue, effective methods are proposed to compute the ROA for partially unknown systems. Lyapunov-based methods are developed and extended to uncertain systems, where a Lyapunov certified ROA (LCROA) estimation is conducted for uncertain, polynomial systems

[14], [15]. Furthermore, learning-based methods have also been studied in the literature. Among these, the use of Gaussian processes (GP) is shown to be a promising approach to quantify the uncertainty in the stochastic process [16, 17]. The idea of uniting SOSP and GP naturally arises to compute the LCROA [18–20].

Inspired by the work in [21] that firstly uses GP to compute the barrier certified ROA (BCROA), based on our previous work in [13, 22], this paper combines SOSPs and GP to estimate the optimal BCROA of partially unknown nonlinear systems. Different from the learned polynomial systems in [20], we use Chebyshev interpolants and polynomial mean functions of GP models to find the optimal BCROA rather than LCROA with relaxed assumptions. The polynomial mean function is proven to be more flexible to match other nonlinear kernels instead of polynomial kernel. To the best of our knowledge, this paper is the first to compute barrier functions via SOSPs in partially unknown nonlinear systems.

The main contributions of this paper are threefold. First, a learned polynomial system is built with probability bounds. Second, an aggressive but safe sample policy is developed to prepare appropriate prior information for higher accuracy of the GP model. Third, a tractable method based on SOSP is proposed to automatically compute the probabilistic optimal BCROA.

2 Preliminary

Consider an autonomous system as follows,

$$\dot{x} = \underbrace{f(x) + g(x)}_{\text{Known}} + \underbrace{d(x)}_{\text{Unknown}}, \quad (1)$$

where $x \in \mathcal{X} \subseteq \mathbb{R}^n$ denotes the state, $f, g : \mathbb{R}^n \rightarrow \mathbb{R}^n$ denote the polynomial and the non-polynomial term respectively, and $d : \mathbb{R}^n \rightarrow \mathbb{R}^n$ denotes the unknown term. All the terms in (1) are Lipschitz continuous.

Without losing generality, systems with a single equilibrium are considered, and this equilibrium could be transformed to the origin via variables substitution [23].

Assumption 1. *The origin ($x = 0$) is a single stable equilibrium of (1), that is $f(0) = g(0) = d(0) = 0$.* \square

To model the system dynamics in a Bayesian framework as developed in [24], we define a prior distribution of noise $[\varepsilon_1, \varepsilon_2, \dots, \varepsilon_k]^T$ over k measurements $[\hat{x}_1, \hat{x}_2, \dots, \hat{x}_k]^T$.

Assumption 2. *The noise $[\varepsilon_1, \varepsilon_2, \dots, \varepsilon_k]^T$ over the system measurements $[\hat{x}_1, \hat{x}_2, \dots, \hat{x}_k]^T$ of (1) is uniformly bound by σ_n , i.e., $\{\varepsilon_i \sim \mathcal{N}(0, \sigma_n^2)\}_{i=1}^k$.* \square

The known dynamical terms $f(x) + g(x)$ can be computed directly. Thus, $d(x)$ can be obtained by subtracting $f(x) + g(x)$ from \dot{x} . In this work, we restrict our attention to the system (1) with bounded $d(x)$:

Assumption 3. *The unknown term $d(x)$ in (1) exists a bounded norm in the reproducing kernel Hilbert space (RKHS), i.e., $\|d(x)\| \leq c_g$, where c_g is a constant.* \square

The RKHS is a Hilbert space of square integrable functions that contains functions of the form $l(x) = \sum_i \alpha_i k(x, x_i)$ as [21] introduced, where $\alpha_i \in \mathbb{R}$ denotes coefficient and $k : \mathcal{X} \times \mathcal{X} \rightarrow \mathbb{R}_0^+$ denotes a symmetric positive definite kernel function of states $x, x_i \in \mathcal{X}$. For more details about the RKHS norm, we kindly refer interested readers to [25].

2.1 Barrier Functions

To introduce the barrier function, let us first consider a simple autonomous system as follows,

$$\dot{x} = f(x), \quad (2)$$

where $f(x)$ is locally Lipschitz continuous and the origin is a single stable equilibrium point. The safety and stability of (2) can be guaranteed by ROA. State trajectories starting inside the barrier function certified ROA (BCROA) $\mathcal{L} = \{x \in \mathcal{X} | h(x) \geq 0\}$ (BCROA) will never enter into the unsafe region $\mathcal{L}_U = \mathcal{X} \setminus \mathcal{L}$ as defined,

$$\begin{aligned} \forall x \in \mathcal{L} \quad & h(x) \geq 0, \\ \forall x \in \mathcal{L}_U \quad & h(x) < 0, \\ \forall x \in \mathcal{L} \quad & \frac{\partial h(x)}{\partial x} \dot{x} \geq 0. \end{aligned} \quad (3)$$

In contrast, the Lyapunov function $V(x)$ certified ROA $\mathcal{L}_V = \{x \in \mathcal{X} | V(x) \leq c\}$ (LCROA), is generated by the sublevel set of $V(x)$ as $\{x | V(x) \leq c\}$, where state trajectories starting inside \mathcal{L}_V will always converge to the origin. Lemma 1 declares a relationship between \mathcal{L} and \mathcal{L}_V .

Lemma 1. *(Lemma 3.2 of [13]) Given an autonomous dynamical system (2) that is asymptotically stable at the origin, the estimate of ROA with barrier function $h(x)$ is no smaller than the estimate of the sublevel set of Lyapunov function $V(x)$, i.e., $\mathcal{L}_V \subseteq \mathcal{L}$.* \square

Algorithms to obtain the Lyapunov maximum sublevel c^* and the optimal barrier function $h^*(x)$ from [13] are introduced in Section 4.1. Example 1 illustrates the expanded \mathcal{L}_V and \mathcal{L} certified by c^* and $h^*(x)$.

Example 1: Consider an autonomous system

$$\begin{bmatrix} \dot{x}_1 \\ \dot{x}_2 \end{bmatrix} = \begin{bmatrix} -x_1^3 - x_1 x_2^2 \\ -x_2 - x_1^2 x_2 \end{bmatrix}. \quad (4)$$

In (4), the LCROA $\mathcal{A}_1 = \{x | V(x) \leq c^* = 1.063\}$ is established by a 4th degree $V(x) = x_1^4 + x_2^4 + x_1^2 x_2^2 + x_1^2 + x_2^2 + x_1 x_2$, and the BCROA $\mathcal{A}_2 = \{x | h^*(x) \geq 0\}$ is computed by another 4th degree polynomial barrier function $h^*(x)$.

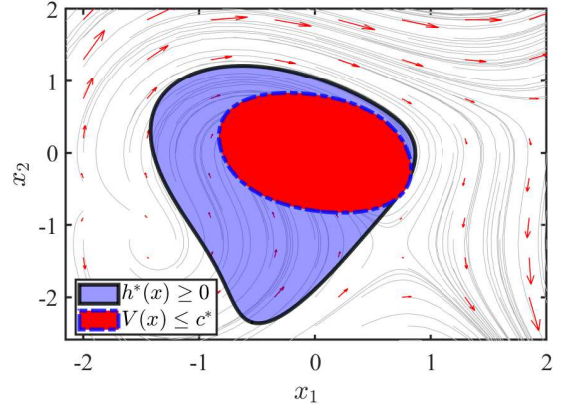


Figure 1: Comparison of the LCROA and BCROA in (4). The red region enclosed by a dashed blue ellipse depicts the estimated LCROA \mathcal{A}_1 , while the light blue region enclosed by the solid black line depicts the BCROA \mathcal{A}_2 .

As shown in Figure 1, \mathcal{A}_2 is significantly larger than \mathcal{A}_1 . Consequently, the BCROA allows more states to be explored. In this paper, we will leverage the barrier function to obtain permissive safety and stability guarantee of system (1).

2.2 Gaussian Processes

Gaussian processes (GP) provide a non-parametric regression method to capture the unknown dynamics in Bayesian framework. In the GP model, every variable is associated with a normal distribution, where the prior and the posterior GP model of these variables obey a joint Gaussian distribution [24]. A GP model is characterized by the mean function

$m(x)$ and the covariance function $cov(x, x')$, where $cov(x, x')$ denotes the similarity between any two states $x, x' \in \mathcal{X}$ based on kernel functions $k(x, x')$. The measurements of $d(x)$ in (1) are used to construct a GP model with polynomial mean functions and various kernel functions as follows.

Proposition 1. *Suppose we have access to the k measurements of $d(x)$ in (1) that satisfy the Assumption 2. Then, the following GP model of $d(x)$ is established with polynomial mean function $m(x_*)$ and covariance function $cov(x, x_*)$ as,*

$$\begin{aligned} m(x_*) &= \varphi(x_*)^T w, \\ cov(x, x_*) &= k(x_*, x_*) - k_*^T (K + \sigma_n^2 I)^{-1} k_*. \end{aligned} \quad (5)$$

where x_* is the query state, $\varphi(x_*)$ is a monomial vector, w is a coefficient vector, $[K]_{(i,j)} = k(x_i, x_j)$ is a kernel Gramian matrix and $k_* = [k(x_1, x_*), k(x_2, x_*), \dots, k(x_w, x_*)]^T$.

Proof. See Appendix. \square

Remark 1. *Proposition 1 supports us to define the degree of polynomial $m(x_*)$ in (5). Besides, it establishes a feasible link between polynomial mean functions and other flexible kernels, including polynomial kernel [20].* \square

3 Learning the Partially Unknown System

In this section, we will discuss Chebyshev interpolants for nonlinear functions approximation. Then, we will express the partially unknown system (1) in polynomial form based on Chebyshev interpolants and GP.

3.1 Chebyshev Interpolants

Chebyshev interpolants provide a useful way to approximate a class of nonlinear functions with a bounded remainder [26]. The term $g(x)$ in (1) can be approximated by the Chebyshev interpolants P_k of degree k in $[-1, 1]$ as,

$$g(x) \approx P_k(x) = \sum_{i=0}^k \alpha_i \tau_i(x) = \langle A, T \rangle, \quad \forall i \in [0, k], \quad (6)$$

where i denotes the subscript of the coefficients vector $A = [\alpha_0, \alpha_1, \dots, \alpha_k]$ and the Chebyshev polynomials vector $T = [\tau_0, \tau_1, \dots, \tau_k]$ that satisfies,

$$\begin{aligned} \alpha_i(x) &= \begin{cases} \frac{1}{\pi} \int_{-1}^1 \frac{g(x) \tau_i(x)}{\sqrt{1-x^2}} dx, & i = 0, \\ \frac{2}{\pi} \int_{-1}^1 \frac{g(x) \tau_i(x)}{\sqrt{1-x^2}} dx, & i \in [1, k], \end{cases} \\ \tau_i(x) &= \cos(i \arccos(x)), \quad \forall i \in [0, k]. \end{aligned} \quad (7)$$

Note that, Chebyshev interpolants are applicable to any arbitrary interval $I = [a, b]$ by the following transformation,

$$I(x) = \frac{2x - (b+a)}{b-a}. \quad (8)$$

We define the remainder $\xi = g(x) - P_k(x)$ based on (6). The following inequality from [26] declares that the remainder ξ of Chebyshev interpolants is bounded over the domain.

Lemma 2. (Theorem 8.2 of [26]) *Let a function $g(x)$ analytic in $[-1, 1]$ be analytically containable to the open Bernstein ellipse E , where it satisfies $|g(x)| \leq m$ for some m . Then, its Chebyshev interpolants $P_k(x)$ satisfies*

$$\forall k \geq 0, \|g(x) - P_k(x)\| \leq \frac{4m\rho^{-k}}{\rho - 1}. \quad \square$$

The Bernstein ellipse E has foci ± 1 and major radius $1 + \rho$ for all $\rho \geq 0$. For more details about the Bernstein ellipses, we kindly refer to the book by Trefethen [26].

Based on Lemma 2, the system (1) can be expressed as,

$$\dot{x} = f(x) + P_k(x) + d_\xi(x), \quad (9)$$

where the unknown term $d_\xi(x)$ satisfies Assumption 2, 3,

$$d_\xi(x) = d(x) + \xi. \quad (10)$$

The approximation accuracy of Chebyshev interpolants is linearly dependent on the degree. We will illustrate a comparison in the following example.

Example 2: Chebyshev interpolants to the non-polynomial function $y = \sqrt{|x-3|}$ of degree 4 and 80 in $[0, 6]$.

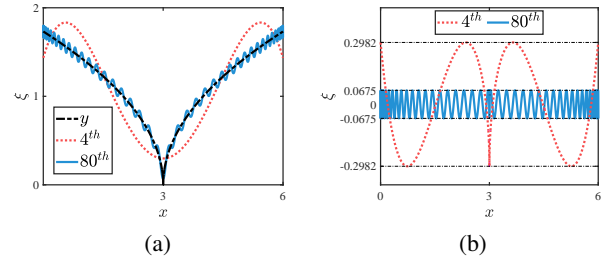


Figure 2: (a) The dashed black line depicts y , the red dot line and the solid blue line depicts the Chebyshev interpolants of degree 4 and 80 respectively. (b) The red dot line and the solid blue line depicts the value of ξ in (10) regarding the Chebyshev interpolants of degree 4 and 80.

As seen in Figure 2, the higher degree of the Chebyshev interpolants is significantly more accurate in the polynomial form, such that we can do further polynomial analysis.

3.2 Probability Bounds on the GP model

The following result provides the probability bounds in the distribution of a GP model.

Lemma 3. (Lemma 2 of [17]) *Suppose we have k measurements $\{(x_1, y_1), (x_2, y_2), \dots, (x_k, y_k)\}$ of a bounded function $h(x) \in \mathcal{H}$, where x denotes the state, y denotes the measurement of $h(x)$ that corrupted with noise $\{\epsilon_1, \epsilon_2, \dots, \epsilon_k\} \sim \mathcal{N}(0, \sigma_n^2)$, and \mathcal{H} denotes the RKHS. Let $\delta \in (0, 1)$. For $h(x)$ and its inferred GP model $(m_h(x), \sigma_h^2(x))$ holds,*

$$\mathbb{P}\{\forall i \in k, |h(x_i) - m_h(x_i)| \leq \sqrt{\beta_k} \sigma_h(x_i)\} \geq (1 - \delta)^k, \quad (11)$$

where $\beta_k = 2\|h\|^2 + 300\gamma_k \log^3(k/\delta)$ is a discounting factor, $\|\cdot\|$ is a norm of \mathcal{H} , and γ_k is a factor denoting the maximum mutual information over the measurements. \square

Remark 2. The value of γ_k is related to the type of kernels, e.g., RBF kernel, Matérn kernel and linear kernel from [27]. Thus, its sublinear dependent term β_k can be regarded as a constant [18]. In [17], a more correlated statement yields that with more appropriate prior information, the value of $\sigma_h(x)$ will decrease such that the dynamics $h(x)$ can be represented by $m_h(x)$ with fewer differences. \square

We can learn the exact value of $d_\xi(x)$ in (10) by using a GP model based on k measurements. Combining previous results of the system (9), a probabilistic statement toward the exact dynamics,

$$\dot{x} = f(x) + P_k(x) + m_{d_\xi}(x), \quad (12)$$

holds with probability greater or equal to $(1 - \delta)^k$, $\delta \in (0, 1)$. A safe sample policy about improving the prior information on GP models will be discussed in next section.

3.3 Covariance Oriented Safe Sample Policy

Computing a high-probability GP model is closely related to the appropriate prior information. If the mean function $m(x)$ of a GP model is closer to the prior information, the value of $cov(x, x_*)$ will decrease to show the higher relevance to the exact dynamics [24]. Therefore, guiding the process to handle the information with higher covariance value will speed up the learning process. We regulate an aggressive sample policy inside an existed ROA to remain the prior information safety over processes as follows,

$$x^* = \underset{x, \psi(t; d_\xi(x)) \in \mathcal{L}_k}{\operatorname{argmax}} \sum_{k=0}^K cov(x, \psi(t; d_\xi(x))), \quad (13)$$

where $\sum cov(x, \psi(t; d_\xi(x)))$ denotes the sum of the covariance value of the trajectory $\psi(t; d_\xi(x))$ starting from a point $x \in \mathcal{L}_k$, \mathcal{L}_k denotes the ROA estimation at each episode, k denotes the index number of the episodes and K denotes the total number of these samples. When the sampling policy (13) exists, the learned system will reduce uncertainty all the time. Example 3 shows a comparison of ROA between the original system (1) and the learned system (12).

Example 3: Consider a partially unknown nonlinear system, where $d(x)$ denotes the unknown term as

$$\begin{bmatrix} \dot{x}_1 \\ \dot{x}_2 \end{bmatrix} = \begin{bmatrix} -x_1 + x_2 \\ x_1^2 x_2 + 1 - \sqrt{|\exp(x_1) \cos(x_1)|} \end{bmatrix} + \begin{bmatrix} 0 \\ d(x) \end{bmatrix}. \quad (14)$$

The non-polynomial term in (14) is approximated by 4th degree Chebyshev interpolants in a compact set $[-2, 2] \times [-2, 2]$. We measure the state trajectory of point $x_0 = (-0.05, -0.05)$ to construct the first learned system with 3rd degree polynomial mean function. Measurements of $d_\xi(x)$ are obtained by subtracting $f(x) + P_k(x)$ in (9). Based on the state trajectory information of $d_\xi(x)$, the learned system is established with ROA and a stable equilibrium point, as shown in Figure 3(b). Following the sample policy (13), some points inside the ROA are used to compute the sum of covariance

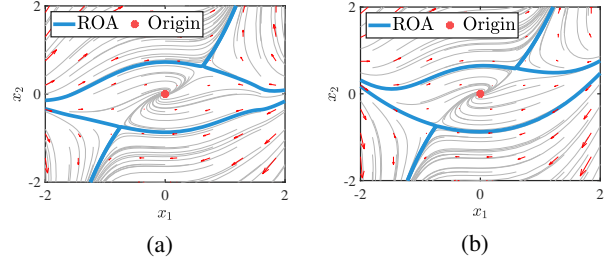


Figure 3: (a) The left schematic demonstrates the ROA of (14) with $d(x) = 0$. (b) The right schematic demonstrates the ROA of the learned polynomial system (12). The blue solid line depicts the exact ROA boundary, and the red filled circle depicts the original point.

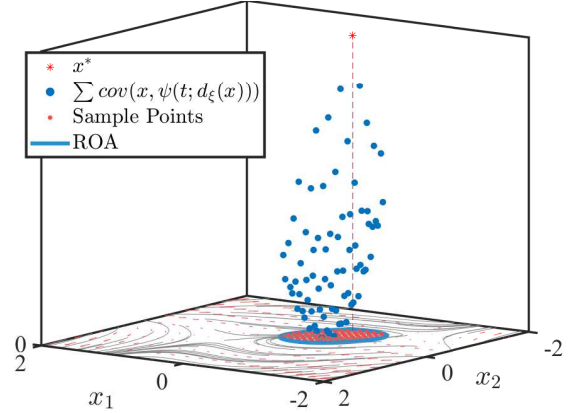


Figure 4: The computation result of $\sum cov(x, \psi(t; d_\xi(x)))$ based on sample points of Figure 3(b). The red star point poses the most uncertain point with maximum value of $\sum cov$, the blue solid points in the space denote the value of $\sum cov$ starting from the red solid points in $x_1 - x_2$ plane and the solid blue ellipse denotes a given ROA \mathcal{L}_k .

value, as seen in Figure 4. Compared to the points close to the edge of ROA, those nearby the origin have smaller sum of covariance value and can be considered with less uncertainty. The distribution of the sum of covariance value poses a direction to trace the most uncertain point in the learned system.

Example 3 shows how we transform the partially unknown system (1) into polynomial form, which paves a way for future SOSP.

4 Estimating the Region of Attraction

In section 4, we will estimate the ROA of the learned polynomial system (12) via SOSPs. The relationship of estimates between the learned polynomial system and the true dynamics will also be discussed.

4.1 Parameterize the ROA by Barrier Function

The parameterization of a barrier function in (12) via SOSPs is developed in [13]. To deal with the non-negativity con-

straints, we will introduce the Positivstellensatz (P-satz) in the following lemma.

Let \mathcal{P} be the set of polynomials and \mathcal{P}^{SOS} be the set of sum of squares polynomials, e.g., $P(x) = \sum_{i=1}^k p_i^2(x)$, where $P(x) \in \mathcal{P}^{\text{SOS}}$ and $p_i(x) \in \mathcal{P}$.

Lemma 4. ([28]) For polynomials $\{a_i\}_{i=1}^m$, $\{b_j\}_{j=1}^n$ and p , define a set $\mathcal{B} = \{x \in \mathcal{X} : \{a_i(x)\}_{i=1}^m = 0, \{b_j(x)\}_{j=1}^n \geq 0\}$. Let \mathcal{B} be compact. The condition $\forall x \in \mathcal{X}, p(x) \geq 0$ holds if the following condition is satisfied,

$$\begin{cases} \exists r_1, \dots, r_m \in \mathcal{P}, s_1, \dots, s_n \in \mathcal{P}^{\text{SOS}}, \\ p - \sum_{i=1}^m r_i a_i - \sum_{j=1}^n s_j b_j \in \mathcal{P}^{\text{SOS}}. \end{cases} \quad \square$$

This lemma declared that any strictly positive polynomial p is in the cone that generated by polynomials $\{a_i\}_{i=1}^m$ and $\{b_j\}_{j=1}^n$. Using Lemma 4, the optimal barrier function $h^*(x)$ of system (2) can be searched using the 3 SOSPs.

1. Obtain the maximum sublevel set $\{x | V(x) \leq c^*\}$ of a specified Lyapunov function $V(x)$ by a bilinear search,

$$\begin{aligned} c^* = & \max_{c \in \mathbb{R}^+, L_c(x) \in \mathcal{P}^{\text{SOS}}} c \\ \text{s.t.} & -\frac{\partial V(x)}{\partial x} \dot{x} - L_c(x)(c - V(x)) \in \mathcal{P}^{\text{SOS}}, \end{aligned} \quad (15)$$

where $L_c(x)$ is an auxiliary factor to relax the non-negativity constraint for the initial barrier function $h(x)$.

2. Search another two auxiliary factors $L_{1,2}(x)$ for $h(x)$,

$$\begin{aligned} & \exists L_1(x), L_2(x) \in \mathcal{P}^{\text{SOS}} \\ \text{s.t.} & -\frac{\partial V(x)}{\partial x} \dot{x} - L_1(x)h(x) \in \mathcal{P}^{\text{SOS}}, \\ & \frac{\partial h(x)}{\partial x} \dot{x} - L_2(x)h(x) \in \mathcal{P}^{\text{SOS}}. \end{aligned} \quad (16)$$

Meanwhile, $h(x)$ can be re-written into the square matrix representation form as $h(x) = Z(x)^T Q Z(x)$, where Q is a semi-definite coefficient matrix and $Z(x)$ is a monomial vector [13]. The trace $Tr(\cdot)$ of Q is used to approximate the volume of barrier certified ROA (BCROA).

3. Enlarge $Tr(Q)$ to parameterize a permissive $h(x)$ with fixed $L_1(x)$ and $L_2(x)$,

$$\begin{aligned} & \max_{h(x) \in \mathcal{P}} Tr(Q) \\ \text{s.t.} & -\frac{\partial V(x)}{\partial x} \dot{x} - L_1(x)h(x) \in \mathcal{P}^{\text{SOS}}, \\ & \frac{\partial h(x)}{\partial x} \dot{x} - L_2(x)h(x) \in \mathcal{P}^{\text{SOS}}. \end{aligned} \quad (17)$$

The optimal barrier function $h^*(x)$ can be found if the increase of $Tr(Q)$ is less than a threshold, otherwise repeat 2 and 3 for a long term.

The SOSPs above demonstrate the details to compute an optimal BCROA in polynomial systems. Thus, if a ROA exists in the learned polynomial system (9), we can compute the ROA via these SOSPs directly.

4.2 Existence of Probabilistic BCROA

The conditions on the existence of a BCROA in the learned system (12) are given in the following result.

Theorem 1. Given k measurements of a partially unknown system (9) such that we can obtain a learned system (12) with probability greater or equal to $(1 - \delta)^k$, $\delta \in (0, 1)$. If there exists a BCROA $\mathcal{L} = \{x \in \mathcal{X} | h(x) \geq 0\}$ in (12) and

$$\frac{\partial h(x)}{x} (f(x) + P_k(x) + m_{d_\xi}(x)) \geq 0 \quad (18)$$

holds for the states $x \in \mathcal{L}$, then \mathcal{L} is a subset of the ROA in (9) with probability bounds $((1 - \delta)^k, 1)$.

Proof. Given an arbitrary initial state $x_0 \in \mathcal{L}$ in the learned system (12), the state trajectory $\psi(t; x_0), t \in [0, \infty]$ is guaranteed to converge to the origin due to the forward invariance. By the definition (3) of barrier function, $\frac{\partial h(\psi(t; x_0))}{\partial t}$ is non-negative over $\psi(t; x_0) \in \mathcal{L}$, such that $h(\psi(t; x_0))$ is strictly increasing along the trajectory $\psi(t; x_0), t \in [0, \infty)$. Thus, $\forall x_0 \in \mathcal{X}$ of (12) generates the barrier certified ROA \mathcal{L} . Since the dynamics of (9) are represented by (12) with probability bounds $((1 - \delta)^k, \delta)$ via the GP model, the BCROA of the approximated system (12) also has the same probability bounds with the ROA of (9), which completes the proof. \square

Theorem 1 shows a tractable condition under which a BCROA can be built by solving an SOSP (a convex optimization problem). It further provides the probability bounds of the generated BCROA and shows the probabilistic relationship with the ROA of the original system (9).

4.3 Probabilistic Optimal BCROA Estimation

In this subsection, we display an algorithm to show the procedures in computing the probabilistic optimal estimate of BCROA. This algorithm is illustrated in Figure 5.

After Algorithm 1, it is time to show another main result of this work:

Theorem 2. Algorithm 1 establishes K probabilistic ROA $[\mathcal{L}_1^*, \mathcal{L}_2^*, \dots, \mathcal{L}_K^*]^T$ with probabilities greater or equal to $[(1 - \delta_1)^{n_1}, (1 - \delta_2)^{n_2}, \dots, (1 - \delta_K)^{n_K}]^T$, where $n_i, i = 1, 2, \dots, K$, is the sample number. Then, the following statements hold:

$$\begin{aligned} \mathbb{P}\{\forall i \in [1, K], \forall \mathcal{L}_i^* \neq \emptyset, \mathcal{L}_\cup^* \subset D\} &= \min_{i=1}^K (1 - \delta_i)^{n_i}, \\ \mathbb{P}\{\forall i \in [1, K], \forall \mathcal{L}_i^* \neq \emptyset, \mathcal{L}_\cap^* \subset D\} &= \max_{i=1}^K (1 - \delta_i)^{n_i}, \end{aligned} \quad (19)$$

where $\mathcal{L}_\cup^* = \cup_{i=1}^K \mathcal{L}_i^*$, $\mathcal{L}_\cap^* = \cap_{i=1}^K \mathcal{L}_i^*$ denotes the largest and smallest region of optimal BCROAs, respectively. D denotes the ROA of the known dynamics of system (1).

Proof. By executing Algorithm 1 with K episodes, we obtain K optimal BCROAs $[\mathcal{L}_1^*, \mathcal{L}_2^*, \dots, \mathcal{L}_K^*]^T$ with probability bounds $[(1 - \delta_1)^{n_1}, 1], [(1 - \delta_2)^{n_2}, 1], \dots, [(1 - \delta_K)^{n_K}, 1]^T$ of

Algorithm 1: Optimal BCROAs Estimation

Input: Original system (1); initial sublevel set of a Lyapunov function $\{x|V(x) \leq c_0\}$; SOS termination ε and episodes K .

Output: Optimal BCROAs $R = [\mathcal{L}_1^*, \mathcal{L}_2^*, \dots, \mathcal{L}_K^*]^T$; probability bounds $P = [\delta_1, \delta_2, \dots, \delta_K]^T$.

- 1 Preprocess (1) into (9) by Chebyshev interpolants. Initialize the prior information set $D_\xi = \emptyset$.
 - 2 Collect the state trajectory $\psi(t; x_0)$ of $x_0 \in \mathcal{L}_0$ for the measurements of $d_\xi(x)$ in (9) as D_0 .
 - 3 **for** $i \in \{1, 2, \dots, K\}$ **do**
 - 4 Update prior information $D_\xi = \cup D_{i-1}$.
 - 5 Construct (12) with polynomial $m(x)$.
 - 6 Execute SOSP (15). Set the initial barrier function as $h_i(x) = c^* - V(x)$.
 - 7 Execute SOSPs (16) and (17) for the optimal BCROA $\mathcal{L}_i^* = \{x|h_i^*(x) \geq 0\}$.
 - 8 Compute the probability bounds. Collect the state trajectory $D_i(x)$ of the most uncertain point as (13) implies.
 - 9 **return** R, P .
-

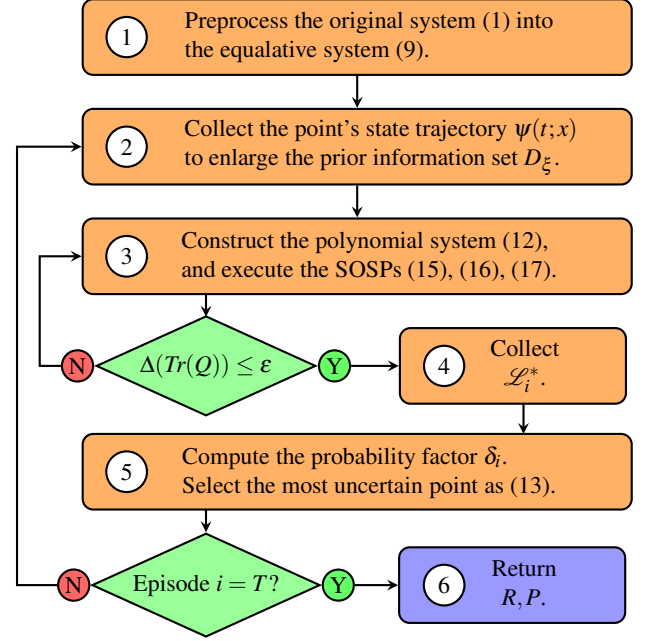


Figure 5: Flowchart of Algorithm 1.

the dynamics in (1) without unknown term. Episode K increases with larger information set D_ξ and smaller probability bounds of the learned system (12). When $K \rightarrow \infty$, GP models can be inferred with the richest D_ξ such that the probability lower bound is $(1 - \delta_K)^{n_K} \rightarrow 1$. Thus, we can relax the condition of K to obtain a conservative probability $1 - \min_{i=1}^K \delta_i$ of \mathcal{L}_\cup^* and a permissive probabilistic $1 - \max_{i=1}^K \delta_i$ of \mathcal{L}_\cap^* separately. \square

Theorem 2 gives the probability of the optimal BCROAs obtained from Algorithm 1. A higher degree of polynomial mean function $m_{d_\xi}(x)$ in (12) could enjoy a higher accuracy of the dynamics. It is worthy noting that the corresponding Lyapunov function $V(x)$ and the barrier function $h(x)$ could increase their degrees simultaneously for a better estimation.

5 Numerical Examples

Two cases are studied using MATLAB 2020a on a laptop with 16GB DDR4 RAM and an Intel Core i5-7300HQ processor. MATLAB toolboxes Chebfun, GPML, SOSOPT, SOS-TOOLS and MOSEK solver toolbox are used for executing Algorithm 1 in this section.

5.1 Example 4: A 2D Nonlinear System

Extended to Example 3, we consider the system:

$$\begin{bmatrix} \dot{x}_1 \\ \dot{x}_2 \end{bmatrix} = \begin{bmatrix} -x_1 + x_2 \\ x_1^2 x_2 + 1 - \sqrt{|\exp(x_1) \cos(x_1)|} \end{bmatrix} + \begin{bmatrix} 0 \\ d(x) \end{bmatrix}. \quad (20)$$

Example 3 shows the construction of the first learned dynamical system and the sample policy (13) in Figure 3(b) and Figure 6, respectively. The noise over measurements is bounded by $\sigma_n = 0.01$. The learned GP models are consisted by a 2^{nd} degree polynomial mean function $m(x)$ with initial value of

zero, and a RBF kernel function $k(x, x') = \sigma_f^2 \exp(-\frac{|x-x'|}{2l^2})$ is considered with signal variances $\sigma_f^2 = \exp(0.1)$ and length scale $l^2 = \exp(0.2)$, where $x, x' \in \mathcal{X}$ in (5).

We then execute Algorithm 1 with 10 episodes. A 4^{th} order $V(x) = 2x_1^4 + 0.5x_2^4 - x_1^2 x_2^2 + x_1^2 + x_2^2 - 0.5x_1 x_2$ with a sublevel set $\{x|V(x) \leq c_0 = 0.1\}$ is considered as a LCROA, to search for the optimal BCROAs \mathcal{L}_{1-10}^* . Besides, we adopt the method in [21] to obtain the probability bounds with a fixed discounting factor $\sqrt{\beta} = 2$. The probability bounds of optimal BCROAs can be obtained as $\mathbb{P}\{\forall \mathcal{L}_{i \in [1, 10]}^*, \mathcal{L}_i^* \subset D\} \in [0.9500, 0.9700]$, where D is the exact ROA of original system.

In Figure 6, each computed optimal BCROA is displayed with a fixed transparency. The smallest optimal BCROA is established with the probability bound $[0.9700, 1]$, while the largest optimal BCROA is established with the probability bound $[0.9500, 1]$. Compared to the given LCROA method, our result based on these optimal BCROAs is obviously larger with precise probabilistic statement.

5.2 Example 5: A 3D Nonlinear System

Consider the 3D nonlinear systems corrupted with two unknown terms $d_1(x), d_3(x)$ as the form of (1),

$$\begin{bmatrix} \dot{x}_1 \\ \dot{x}_2 \\ \dot{x}_3 \end{bmatrix} = \begin{bmatrix} -x_1^2 - \cos(x_1^2) \sin(x_1) \\ -x_2 - x_1^3 x_2 \\ -x_1^2 x_3 + 1 - \sqrt{|\exp(x_1) \cos(x_1)|} \end{bmatrix} + \begin{bmatrix} d_1(x) \\ 0 \\ d_3(x) \end{bmatrix}. \quad (21)$$

The non-polynomial terms in (21) are approximated by the 4^{th} degree Chebyshev interpolants in $[-2, 2] \times [-2, 2] \times [-2, 2]$. To learn the system dynamics, we first collect the state trajectory of the point $(-0.1, -0.1, 0.1)$, where the

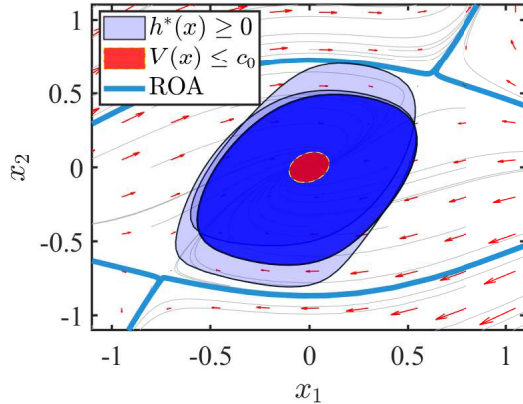


Figure 6: ROA estimation of (20). The red region enclosed by the yellow dashed ellipse depicts the maximum sublevel of $V(x)$ certified LCROA and the blue region enclosed by the solid black line denotes the optimal BCROA. The gray solid lines and the red arrows depict the vector field of (20) without unknown term.

Table 1: Computation Time t_c [sec] of Algorithm 1.

	Episode 1	Episode 5	Episode 10
Example 4	35.6	168.3	1752.6
Example 5	406.4	837.8	1329.4

noises over $d_1(x)$ and $d_3(x)$ are bounded by $\sigma_n = 1 \times 10^{-2}$. The learned GP models are consisted of a 3rd degree polynomial mean function $m(x) = 0$ initially and a RBF kernel with $\sigma_f^2 = \exp(0.01)$ and $l^2 = \exp(0.2)$.

Algorithm 1 is executed 10 times for this example with a 4th order $V(x) = 10x_1^4 + x_2^4 + 20x_3^4 + 2x_1^2x_2^2 - 4x_3^2x_2^2 + 3x_1^2x_3^2$ and its sublevel set $\{x | V(x) \leq c_0 = 5 \times 10^{-3}\}$. Again, set $\sqrt{\beta} = 2$ such that the probability bounds of these optimal BCROAs can be computed as $\mathbb{P}\{\forall \mathcal{L}_{i=1}^{10}, \mathcal{L}_i \subset D\} \in [0.8395, 0.9567]$, where D is the exact ROA of (21).

The generated optimal BCROAs are displayed in Figure 7 with a fixed transparency. Again, the optimal BCROA method obtains a better estimation compared to the LCROA method. With fixed GP iteration time 1000, Table 1 shows these two examples' computation time over Algorithm 1 at the certain episode.

6 Conclusion

In this work, we propose a theoretical method to compute a barrier certified region of attraction such that the stability and safety can be both guaranteed for a class of partially unknown systems. We also propose an algorithm based on Chebyshev interpolants, Gaussian processes, sum-of-squares programming and a safe sampling policy. The computation efficiency of the proposed algorithm has been demonstrated via two numerical examples in searching for the optimal barrier certified region.

Despite the aforementioned computational efficiency, we

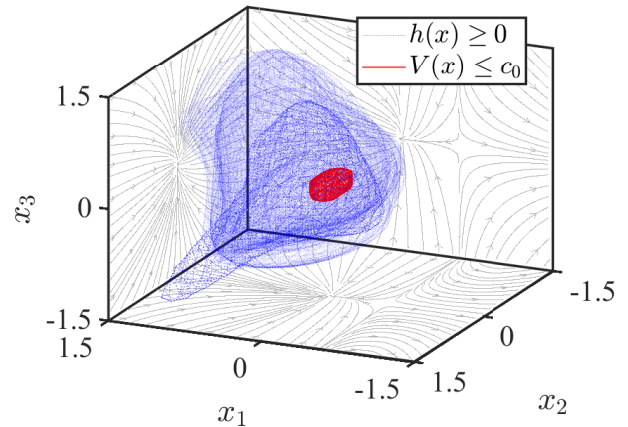


Figure 7: ROA estimations of (21). The red cube enclosed by the solid lines depicts the given LCROA and the blue cube enclosed by the dashed line denotes the optimal BCROAs. The vector field is projected onto the planes.

have to admit that a large amount of unknown terms may affect the accuracy and efficiency of proposed algorithm. Possible solutions to address this issue could be a systematic way of constructing an efficient sampling policy [29] or focusing on local GP regression [30]. Thus, future efforts will be devoted to prior data selection, and controller design for further enlarging the estimated region of attraction for partially unknown systems [13, 17].

References

- [1] E. Glassman, A. L. Desbiens, M. Tobenkin, M. Cutkosky, and R. Tedrake, "Region of attraction estimation for a perching aircraft: A Lyapunov method exploiting barrier certificates," in *Proceedings of the International Conference on Robotics and Automation*, pp. 2235–2242, 2012.
- [2] L. Wang, E. A. Theodorou, and M. Egerstedt, "Safe learning of quadrotor dynamics using barrier certificates," in *Proceedings of the International Conference on Robotics and Automation*, pp. 2460–2465, 2018.
- [3] S.-C. Hsu, X. Xu, and A. D. Ames, "Control barrier function based quadratic programs with application to bipedal robotic walking," in *Proceedings of the American Control Conference*, pp. 4542–4548, 2015.
- [4] P. Magne, D. Marx, B. Nahid-Mobarakeh, and S. Pierfederici, "Large-Signal Stabilization of a DC-Link Supplying a Constant Power Load Using a Virtual Capacitor: Impact on the Domain of Attraction," *IEEE Transactions on Industry Applications*, vol. 48, no. 3, pp. 878–887, 2012.
- [5] G. Chesi, *Domain of attraction: Analysis and control via SOS programming*, vol. 415. Springer Science & Business Media, 2011.
- [6] V. I. Zubov, *Methods of AM Lyapunov and their application*. P. Noordhoff, 1964.
- [7] F. Blanchini, "Set invariance in control," *Automatica*, vol. 35, no. 11, pp. 1747–1767, 1999.
- [8] A. D. Ames, S. Coogan, M. Egerstedt, G. Notomista, K. Sreenath, and P. Tabuada, "Control barrier functions: The-

- ory and applications,” in *Proceedings of the European Control Conference*, pp. 3420–3431, 2019.
- [9] A. D. Ames, X. Xu, J. W. Grizzle, and P. Tabuada, “Control barrier function based quadratic programs for safety critical systems,” *IEEE Transactions on Automatic Control*, vol. 62, no. 8, pp. 3861–3876, 2016.
- [10] P. A. Parrilo, *Structured semidefinite programs and semialgebraic geometry methods in robustness and optimization*. PhD thesis, California Institute of Technology, 2000.
- [11] I. R. Manchester, M. M. Tobenkin, M. Levashov, and R. Tedrake, “Regions of attraction for hybrid limit cycles of walking robots,” *IFAC Proceedings Volumes*, vol. 44, no. 1, pp. 5801–5806, 2011.
- [12] A. El-Guindy, D. Han, and M. Althoff, “Estimating the region of attraction via forward reachable sets,” in *Proceedings of the American Control Conference*, pp. 1263–1270, 2017.
- [13] L. Wang, D. Han, and M. Egerstedt, “Permissive barrier certificates for safe stabilization using sum-of-squares,” in *Proceedings of the American Control Conference*, pp. 585–590, 2018.
- [14] D. Han, and M. Althoff, “On estimating the Robust Domain of Attraction for uncertain non-polynomial systems: An LMI approach,” in *Proceedings of the Conference on Decision and Control*, pp. 2176–2183, 2016.
- [15] A. Iannelli, A. Marcos, and P. Seiler, “An equilibrium-independent region of attraction formulation for systems with uncertainty-dependent equilibria,” in *Proceedings of the Conference on Decision and Control*, pp. 725–730, 2018.
- [16] J. Vinogradska, B. Bischoff, D. Nguyen-Tuong, and J. Peters, “Stability of controllers for Gaussian process dynamics,” *The Journal of Machine Learning Research*, vol. 18, no. 1, pp. 3483–3519, 2017.
- [17] J. Umlauf, L. Pöhler, and S. Hirche, “An uncertainty-based control Lyapunov approach for control-affine systems modeled by Gaussian process,” *IEEE Control Systems Letters*, vol. 2, no. 3, pp. 483–488, 2018.
- [18] F. Berkenkamp, R. Moriconi, A. P. Schoellig, and A. Krause, “Safe learning of regions of attraction for uncertain, nonlinear systems with Gaussian processes,” in *Proceedings of the Conference on Decision and Control*, pp. 4661–4666, 2016.
- [19] J. Umlauf, A. Lederer, and S. Hirche, “Learning stable Gaussian process state space models,” in *Proceedings of the American Control Conference*, pp. 1499–1504, 2017.
- [20] A. Devonport, H. Yin, and M. Arcaç, “Bayesian safe learning and control with sum-of-squares analysis and polynomial kernels,” in *Proceedings of the Conference on Decision and Control*, pp. 3159–3165, 2020.
- [21] P. Jagtap, G. J. Pappas, and M. Zamani, “Control barrier functions for unknown nonlinear systems using Gaussian processes,” in *Proceedings of the Conference on Decision and Control*, pp. 3699–3704, 2020.
- [22] D. Han, and M. Althoff, “Estimating the domain of attraction based on the invariance principle,” in *Proceedings of the Conference on Decision and Control*, pp. 5569–5576, 2016.
- [23] H. K. Khalil, *Nonlinear systems; 3rd ed.* Prentice-Hall, 2002.
- [24] C. K. Williams and C. E. Rasmussen, *Gaussian processes for machine learning*, vol. 2. MIT press, 2006.
- [25] V. I. Paulsen and M. Raghupathi, *An introduction to the theory of reproducing kernel Hilbert spaces*, vol. 152. Cambridge university press, 2016.
- [26] L. N. Trefethen, *Approximation Theory and Approximation Practice*. SIAM, 2019.
- [27] N. Srinivas, A. Krause, S. M. Kakade, and M. Seeger, “Gaussian process optimization in the bandit setting: No regret and experimental design,” *arXiv preprint: 0912.3995*, 2009.
- [28] M. Putinar, “Positive polynomials on compact semi-algebraic sets,” *Indiana University Mathematics Journal*, vol. 42, no. 3, pp. 969–984, 1993.
- [29] J. Umlauf, T. Beckers, A. Capone, A. Lederer, and S. Hirche, “Smart forgetting for safe online learning with Gaussian Processes,” in *Learning for Dynamics and Control*, pp. 160–169, PMLR, 2020.
- [30] D. Nguyen-Tuong, M. Seeger, and J. Peters, “Model learning with local Gaussian Process regression,” *Advanced Robotics*, vol. 23, no. 15, pp. 2015–2034, 2009.
- [31] C. Santoyo, M. Dutreix, and S. Coogan, “A barrier function approach to finite-time stochastic system verification and control,” *Automatica*, vol. 125, p. 109439, 2021.
- [32] H. König, *Eigenvalue distribution of compact operators*, vol. 16. Birkhäuser, 2013.

Appendix: Proof of Proposition 1

Proof. Given the definitions of the unknown term $d(x)$ and the measurement $y(x)$ that satisfy Assumption 2 as follows,

$$d(x) = \phi(x)^T w, \quad y(x) = d(x) + \varepsilon, \quad (22)$$

where $\phi(x)$ is a kernel basis vector and w is a weight vector. Mercer’s Theorem [32] allows us to decompose the kernel function with a kernel basis function $\phi(\cdot)$, e.g., the RBF kernel $k(x, x')$ can be decomposed as,

$$\begin{aligned} k(x, x') &= \sigma^2 \exp\left(\frac{(x-x')^2}{-2l^2}\right) \\ &= \sum_{i=0}^{\infty} \frac{\sigma^2 2^i}{2l^2 i!} \exp\left(\frac{(x-x')^2}{-2l^2}\right) \left(\frac{x-x'}{2l^2}\right)^i \exp\left(\frac{(x-x')^2}{-2l^2}\right) \left(\frac{x-x'}{2l^2}\right)^i \\ &= \phi(x)^T \phi(x'), \end{aligned} \quad (23)$$

where σ is the signal variance and l is the length scale. The infinite dimensional kernel basis vector $\phi(x)$ in (23) is,

$$\phi(x) = \exp\left(\frac{(x-x')^2}{-2l^2}\right) \cdot \left(\sqrt{\frac{\sigma^2 2^0}{2l^2 0!}} \left(\frac{x-x'}{2l^2}\right)^0, \sqrt{\frac{\sigma^2 2^1}{2l^2 1!}} \left(\frac{x-x'}{2l^2}\right)^1, \dots\right). \quad (24)$$

We define $p(w) \sim \mathcal{N}(0, \sigma_p^2)$ and $p(\hat{w})$ as the prior distribution and the posterior distribution of w separately, which can be inferred in these forms below,

$$\text{posterior} = \frac{\text{likelihood} \times \text{prior}}{\text{marginal likelihood}}, \quad p(\hat{w}|y, x) = \frac{p(y|x, w) \cdot p(w)}{p(y|x)}. \quad (25)$$

Let $p(\hat{w}|y, x)$ be the posterior distribution of w based on the value of y and x . Let K_1 be the weight-independent marginal likelihood $p(y|x)$. GP is relocating likelihood $p(y|x, w)$ with these k measurements $[(x_1, y_1), (x_2, y_2), \dots, (x_k, y_k)]^T$ in the following formulation

$$p(y|x, w) = \prod_{i=1}^k p(y_i, x_i, w) = \prod_{i=1}^k \frac{\exp\left(\frac{(y_i - \phi(x_i)^T w)^2}{-2\sigma_n^2}\right)}{\sigma_n \sqrt{2\pi}}, \quad (26)$$

to obtain the posterior distribution $p(w|y, x)$,

$$\begin{aligned} p(w|x, y) &= \frac{\prod_{i=1}^k p(y_i, x_i, w) \cdot \frac{1}{\sqrt{2\pi\sigma_p^2}} \exp\left(\frac{w^T \sigma_p^{-2} w}{-2}\right)}{K_1} \\ &= K_2 \cdot \exp\left(\frac{w^T \sigma_p^{-2} w}{-2}\right) \cdot \exp\left(\frac{\sum_{i=1}^k (y_i - \phi(x_i))^T w}{-2\sigma_n^2}\right), \end{aligned} \quad (27)$$

where $K_2 = \frac{1}{K_1 \cdot \sqrt{2\pi\sigma_p^2} \cdot (\sigma_n \sqrt{2\pi})^k}$.

By using the Maximum a Posterior estimation, the exact value of the optimal weight \hat{w} can be obtained as,

$$\begin{aligned} \hat{w} &= \arg \max_w p(w|x, y) = \arg \max_w \log p(w|x, y) \\ &= \arg \min_w -\log p(w|x, y) \\ &= \arg \min_w -\log K_2 + \frac{w^T \sigma_p^{-2} w}{2} + \frac{\sum_{i=1}^k (y_i - \phi(x_i))^T w}{2\sigma_n^2} \\ &= \arg \min_w w^T (\sigma_n^2 \sigma_p^{-2}) w + \sum_{i=1}^k (y_i - \phi(x_i))^T w \\ &= \arg \min_w w^T (\phi(x)^T \phi(x) + \sigma_n^2 \sigma_p^{-2}) w - 2w^T \phi(x)^T y + y^T y \\ &= \arg \min_w L(w). \end{aligned} \quad (28)$$

We can directly compute the partial derivative of the $L(w)$ to find the minimum value of $L(w)$ in (28)

$$\frac{\partial L(w)}{\partial w} = 2(\phi(x)^T \phi(x) + \sigma_n^2 \sigma_p^{-2}) w - 2\phi(x)^T y. \quad (29)$$

Then the updated weight \hat{w} can be parameterized directly,

$$\begin{aligned} \hat{w} &= (\phi(x)^T \phi(x) + \sigma_n^2 \sigma_p^{-2})^{-1} \phi(x)^T y \\ &= \phi(x)^T (\phi(x) \phi(x)^T + \sigma_n^2 \sigma_p^{-2})^{-1} y \\ &= \sigma_p^2 \phi(x)^T (\phi(x) \sigma_p^2 \phi(x)^T + \sigma_n^2)^{-1} y. \end{aligned} \quad (30)$$

Thus, based on the definition of $d(x)$ in (22), we can obtain the predictive output $d(x_*)$ of the query states x_* with the optimal posterior weight \hat{w} ,

$$\begin{aligned} d(x_*) &= \phi(x_*)^T \hat{w} \\ &= \phi(x_*)^T (\sigma_p^2 \phi(x)^T (\phi(x) \sigma_p^2 \phi(x)^T + \sigma_n^2)^{-1} y). \end{aligned} \quad (31)$$

Note that, $\phi(x)$ in (26) can be replaced by a monomial vector $\varphi(x)$ while the processes from (26) to (31) will not be influenced. This will reshape the mean function but do not impact the other variables as follows,

$$\begin{aligned} m(x_*) &= \varphi(x_*)^T \hat{w}, \\ \sigma^2(x_*) &= k(x_*, x_*) - k_*^T (K + \sigma_n^2 I)^{-1} k_*. \end{aligned} \quad (32)$$

where $\varphi(x_*)$ is a monomial vector, \hat{w} is the corresponding posterior weight, $[K]_{(i,j)} = k(x_i, x_j)$ is a kernel Gramian matrix and $k_* = [k(x_1, x_*), k(x_2, x_*), \dots, k(x_w, x_*)]^T$ [24]. Thus, Proposition 1 is obtained, which completes the proof. \square